IEEE Access
Multidisciplinary | Rapid Review | Open Access Journal

Received 8 September 2024, accepted 13 October 2024, date of publication 17 October 2024, date of current version 8 November 2024.

Digital Object Identifier 10.1109/ACCESS.2024.3482434

RESEARCH ARTICLE

Block-Based Adaptive Compressed Sensing by Using Edge Information for Real-Time Reconstruction

V. PAVITRA, (Member, IEEE), AND V. B. S. SRILATHA INDIRA DUTT
Department of Electrical, Electronics and Communication Engineering, GITAM Deemed to be University, Visakhapatnam 530045, India
Corresponding author: V. Pavitra (velagapudipavithra@gmail.com)

ABSTRACT Adaptive Block-Based Compressed Sensing (ABCS) enables optimization of image and video sensing platforms with limited resources, using novel algorithms for efficient reconstruction and real-time operations. Taking number of measurements adaptively based on information contained in each block of the image, results in better quality of recovered image, and is paving ways for general purpose use of compressed sensing in various applications. Some of the major challenges in ABCS are, complexity introduced at encoder end for adaptive rate allocation and choosing or learning a measurement matrix for each allocation rate. As part of this paper, we introduce a novel adaptive measurement allocation technique based on edge information with in the block. The algorithm is further improved by giving special considerations for edges present at the block boundary. DCT (Discrete Cosine Transform) dictionaries are used for measurement and recovery. Using simple encoding for measurement allocation greatly reduces the complexity of encoder network in this scheme. Recovery is done by simple IDCT (Inverse Discrete Cosine Transform) in case of DCT dictionaries. This approach demonstrates high effectiveness without the need for computationally expensive GPU-based training. To assess the network's generalizability, we conducted tests using both natural and medical images. Remarkably, the method exhibited consistent accuracy across various measurement rates in both scenarios. The recovery time for compressively sensed images, whether they are natural or medical, is real-time, with an average duration of around **50-65 milliseconds**. The algorithm is also used in conjunction with Content Aware Scalable deep compressed sensing Network (CASNET) to get learned matrix for measurements on encoder side and pretrained model for reconstruction on decoder side. Proposed method not only converges in constant time across blocks in contrary to the rate allocation method of CASNET, but also outperforms the recovery quality in lower measurement rates. Extensive experimental results shows that proposed algorithm out performs other state of the art algorithms recovery.

INDEX TERMS Adaptive block based compressive imaging, rate allocation, compressed sensing, random sensing matrices, learned sensing matrices, deep compressed sensing.

I. INTRODUCTION

The rapid increase of sensors and sensing systems in current period of time has fueled a digital revolution. This technological advance has yielded huge amounts of high-resolution data. However, managing and storing such massive volumes of information is a big challenge. Thus, there is a need for solutions that can efficiently reduce transmitted data or offer substantial capacity for storage. Various approaches have been devised and embraced to address this demand. Compression of the sensed data thus, is of paramount importance in current day world. Traditional signal processing follows the Shannon-Nyquist theorem. The theorem states that signal or image acquisition should occur at a rate at least twice the highest frequency of the signal. In practice, because of the sheer volume of data generated by sensors, traditional approaches become ineffective and expensive. For instance, JPEG compression, while effective, can be resource-intensive

The associate editor coordinating the review of this manuscript and approving it for publication was Yeon-Ho Chung.

and time-consuming. As sensor technology continues to evolve, striking a balance between data fidelity and efficiency becomes even more critical. To accommodate ever expanding sensor data, innovations in compression algorithms and storage systems are essential. Contrary to traditional methods that adhere to the Shannon-Nyquist theorem, compressed sensing (CS) allows us to capture data at a lower rate by taking few measurements while still ensuring accurate image recovery.

Compressed sensing (CS) is a groundbreaking approach that capitalizes on the compressibility and sparsity of signals, in specific transform domains, to reduce the required measurements. Sparse representations of signals allow us to explore high-dimensional data and uncover underlying structures. By exploiting the inherent sparsity of signals: even with fewer measurements, original image can be reconstructed even in presence of noise [1]. CS recovery is backed by strong mathematical guarantees.

However, CS comes with certain limitations:

Non-Adaptive Random Projection: CS applies non-adaptive random projection for measurement vectors. The direction of projection is random, due to which the efficiency of recovery can be affected [2].

Uniform Energy Contribution: In traditional CS algorithms, all signal components contribute with equal probability and contribute the same energy. This uniform distribution may be sub optimal for few scenarios.

Quality vs. Measurement Trade-Off: Achieving high-quality signal recovery with minimal measurements continue to be a major challenge.

Complex Recovery Process: While CS simplifies compression during acquisition, the subsequent recovery process is resource-intensive.

These challenges limit the widespread adoption of CS technology for general purposes.

To address the limitations of traditional CS, BCS (Block Compressed Sensing) is used in literature [3].

In BCS, the image is divided into blocks which are non-overlapping, and each of the block is processed independently. In contrast, traditional compressive sensing processes the entire image and collects measurements using a single measurement matrix, which can be computationally intensive. In contrast, BCS simultaneously processes these blocks using the measurement matrix. This approach captures the structural aspects of all parts of the image effectively, and aids in better reconstruction.

BCS removes constraints on resources and grants the ability to sense and process images of any dimension. Thus, BCS makes itself adaptable to various practical scenarios.

Like traditional CS, BCS also employs a wide variety of recovery algorithms. OMP (Orthogonal matching pursuit), Matching pursuit and (COSaMP) compressive sampling matching pursuit [4], [5] are few examples for greedy algorithms used for recovery. Using right measurement matrix plays a pivotal role in effectively using CS. BCS employs matrices like Bernoulli, Toeplitz, Gaussian, partial Hadamard, partial Fourier and sparse binary random matrix. These matrices must satisfy the Restricted Isometry Property (RIP) to ensure accurate signal reconstruction. The RIP ensures that the matrix preserves the sparsity of the signal during the sensing process [6].

BCS is very effective when compared to traditional CS in capturing measurements across blocks in the image. However, there are some challenges with BCS algorithms. When processing the image as a whole, contains lot of repetitive structures and sparsity. The blocks in BCS do not have the same level of compression ratio/ sparsity. BCS can enable parallel processing of blocks hence achieve faster recovery. Many times, blocking artifacts are observed in recovered image since inter block relationships are often ignored due to abrupt transitions between adjacent blocks.

Adaptive Block based Compressive Sensing (ABCS) is a remarkable advancement in BCS, as it tackles the challenges posed by traditional methods. ABCS dynamically allocates measurements to each image block based on the presence of information in it. Some blocks may predominantly contain background (low information), while others hold significant details (high information). While assigning higher measurement rates to informative blocks and lower rates to less critical blocks, ABCS maintains an overall measurement rate and balances efficiency and fidelity [7].

ABCS effectively captures the most significant information across all blocks. This adaptability ensures that essential details are preserved while optimizing data acquisition. However, it also increases the encoder complexity and acquisition time by introducing rate allocation algorithms at encoder side. There is a need to maintain N- number of random matrices, one for each allocated rate and to be sent to decoder as well in order to recover corresponding image block.

This problem is solved by various approaches in literature. Certain techniques opt for a fixed number of measurement variations. In this scenario, a predetermined set of random matrices are learned and maintained against these measurement rates. This simplifies the process by avoiding dynamic matrix generation [8]. CASNET, creates a huge learned dictionary [9], where a sub part of it is used as measurement matrix based on allocation rate.

Few methods employ deterministic matrices like Hadamard, 2D DCT (Discrete Cosine Transform), or DWT (Discrete Wavelet Transform) for taking measurements. These matrices cater to the problem by providing predictable and structured measurement patterns. Despite the non-RIP compliance of the ensuing measurement matrix in these cases, the L-DCT-ZZ [10] algorithms utilize, low-pass, 2D Discrete Cosine Transform (2D-DCT) matrices for measurement. Since the transform coefficients' location is known, enables for trivial recovery of image blocks using the 2D IDCT in mere milliseconds.

We summarized the existing ABCS algorithms, in following sections, and also proposed novel adaptive rate allocation algorithm and tested it against both natural and medical images.

A. CONTRIBUTIONS

As part of this paper, we proposed a novel adaptive block based compressive sensing algorithm by using edge information in the block. The proposed algorithm is further improved by adding extra weight in blocks containing edge pixels in block borders. This ensures reduced blocking artifacts in recovered image.

The proposed model is tested against standard data sets of natural images as well as medical images using standard 2D DCT dictionaries. PSNR (Peak Signal to Noise Ratio) and SSIM (Structural Similarity Index Measurement) of recovered images are compared. The method's performance is consistent for both natural as well as medical images. The recovery time of each image is also captured.

The proposed method is further tested against CASNET [9] recovery. In CASNET the rate allocation algorithm is based on a light weight CNN (Convolution Neural Network). This is replaced by proposed method which does not require any GPU or high accelerated processor. The performance of proposed measurement algorithm is superior to CASNET in lower measurement rates.

B. ORGANISATION OF PAPER

Section II Introduces Compressed sensing theory and explores the related work done in the field of CS and DCS (Deep Compressive Sensing). In Section III, we explore, Adaptive Block Compressive Sensing (ABCS) algorithms. Sections IV presents the Edge based Adaptive Rate Allocation (EARA) algorithm and its improvement for special consideration of border pixels WEARA (Weighted Edge based Adaptive Rate Allocation). The empirical investigations are presented in Section V, where we compare these algorithms with other adaptive CS methods. Additionally, the algorithm is tested against DCS algorithm CASNET. Finally, Section VI provides conclusions drawn from the study and future scope.

II. COMPRESSIVE SENSING AND RELATED WORK

The theory of compressed sensing is introduced in this section. Related work done in CS recovery in BCS and DCS approaches are also presented.

A. COMPRESSED SENSING THEORY

CS theory suggests to take measurements instead of samples for direct compression at the time of sensing. Consider an image f which is an N *N dimensional according to Shannon-Nyquist theorem. That means, to capture all details of f, at least N*N samples to be taken. Many signal encoding methods leverage the sparsity of the signal or image in some domain and compress it after acquisition. Compressive sensing builds on the same point that almost all the images/ signals are sparse in some domain. Let ψ be an ortho normal basis in which f is sparse such that

$$f = \psi x \tag{1}$$

where x is K sparse and K≪N. By taking M measurements (M>K by small factor) from the image using a measurement matrix ϕ, the sparsity of x is randomly projected through the measurements.

$$y = \phi x \tag{2}$$

At recovery end, $\hat{x}$ is reconstructed by l_0 minimization and $\tilde{f}$ can be reconstructed back from $\hat{x}$ by using reverse transformation on basis ψ. But in practical scenarios l_0 minimization is challenging. According to Cades and Tao [1] l_0 minimization can be replaced with l_1 minimization, as long as measurement matrix ϕ satisfies RIP (Restricted Isometry Property). Equation (3) show the recovery of $\hat{x}$ from l_1 minimization.

$$\hat{x} = argmin||x||_1; s.t\frac{1}{2}\|(y - \phi x)\|_2^2 \leq \epsilon \tag{3}$$

B. COMPRESSED SENSING RECOVERY METHODS

There are various algorithms proposed in literature for CS recovery. Non-neural-network based solvers are basically optimization algorithms which try to solve the convex optimization problem. Recovery of X is generally done based on equation (4) where algorithms use some regularization term.

$$\hat{x} = \underset{x}{argmin}\frac{1}{2}\|(y - \phi x)\|_2^2 + \lambda R(x) \leq \epsilon \tag{4}$$

where λR is a prior with λ as regularization term. Some of the famous algorithms in this category include ADMM (Alternate Direction of Method of Multipliers), ISTA (Iterative Soft Thresholding Algorithm), AMP (Approximate Message Passing) and TV (Total Variation) based algorithms [11], [12] [13]. Some of the algorithms use Bayesian priors [14], [15] [16]. Edge CS [17] proposes the use of edges information to aid in overall reconstruction of the original image.

With advancement of deep learning models and Nural networks, there are CS recovery algorithms proposed that uses neural network architectures. There are native neural network implementations as well as neural networks formed by unfolding iterative algorithms. CNN based neural network is proposed in MD-Recon-Net [18], CSNET+ [19], [20], CNN With Attention [20]. OPINE-NET [21], ADMM-CSNET [22], ISTA-NET+ [23] and AMP-NET [24] are some examples of neural network based unfolded iterative algorithms. In these networks, neural network translations of the state of art iterative algorithms are unfolded and trained end to end. Most of these recent Deep learning based iterative CS algorithms propose end to end learning and optimization of Neural network along with the sampling matrix. Reference [25] gives review of various CS recovery algorithms.

Block based Compressive Sensing, increased the generalizability of CS by catering to images of any dimension. It divides the image into non overlapping blocks and take measurements from each block. There are number of CS recovery algorithm proposed in literature based on BCS. For example, AMP-NET, ADMM-CSNET and ISTA-NET+ also uses BCS and recovers the image blocks and combines them

back to an image. Since inter block relationships are not considered in these methods, blocking artifacts are observed in the recovered image. Various schemes are used in literature to overcome blocking artifacts. AMP Net uses De-blocker module, a BM3D based filter is used in DR2Net [26] to remove the blocking artifacts. BCS-net uses partial image block recovery and a deep full image recovery to remove blocking artifacts.NL-CSNet [27] uses Non local self-similarity scores to capture long as well as short distance block relationships.

There are majorly 2 issues in these block-based deep CS networks. Rate allocation is flat and does not depend on the information present in each block. Another issue is, each network is trained against each of standard measurement rate and resultant measurement matrix is stored. This requires the network to be trained for n- number of measurement rates which is complex and costly.

The first problem is addressed by Adaptive BCS in literature.

BCS-NET uses adaptive rate allocation by creating few channels and each channel handling a particular measurement rate. The problem with this approach is, only few measurement rates are being considered as the number of channels cannot be huge. You et al. [28] proposed a network to handle the arbitrary number of sampling matrices. However, this method needs huge number of sampling matrices for different measurement rates during training, which makes training process expensive. The next section discusses ABCS algorithms, in which most of them uses deterministic 2D DCT or wavelet dictionaries for measurement and reconstruction.

III. ADAPTIVE BLOCK BASED COMPRESSED SENSING ALGORITHMS

Apart from non-neural network based iterative methods and Neural network based Deep compressed sensing methods which uses fixed number of measurements across blocks, there are some methods proposed in literature that will allocate measurement rate adaptively based on some measure of information present in each of the image block.

Gao et al. [29] proposed adaptive BCS measuring different measurement rates to different blocks, based on sub image characteristics. In [30] adaptive rate allocation per block is proposed based on statistical information like Number of significant DCT coefficients in the block, entropy and variance. Measurements are readjusted to reach overall measurement rate. However, the number of measurements cannot be beyond a particular level in each block, causing ineffective recovery. Among the proposed information, Number of DCT coefficients is the dimension that is always yielding a good result. Zhang et al. [31] proposed a method of measurement rate allocation based on standard deviation. The method is simple and there is no fixed number of measurement limit. However, the effectiveness of the method depends on block size and generally shows good results between measurement rates of 30% to 50%.

Li et al. [32] proposed measurement rate per block allocated based on calculating error between blocks. If the error between adjacent blocks is high, it is considered as more spatial changes between image blocks and allocates more measurements. Though blocking artifacts are reduced by this scheme, the cost involved in hardware implementation of the algorithm proposed at the encoder side is huge.

Algorithm in [33] allocates measurement rates based on texture contrast with in the block. More measurements are taken for higher textual contrast blocks. The model shows consistent high performance across the channels, however, global weighted reconstruction model used increases the recovery complexity.

Zhou et al. [34] proposed a saliency based adaptive partitioning method. Generally, in ABCS the block size is fixed, and only number of measurements will vary based on some measure of information. But in this scheme, the block size is adaptive based on the saliency of the image. This is done by using K means clustering. The major issue with this approach is the complexity introduced both on encoder as well as decoder side due to adaptive block size.

Most of the ABCS algorithms discussed uses deterministic dictionaries for taking measurements. Especially most of them use DCT based measurements. LL-DCT-ZZ algorithm, is the linear and non-adaptive 2D-DCT CS technique. The algorithm draws inspiration from work mentioned in [10] done by Romberg, which observes that compressive sensing (CS) of images is challenging. To aid faster and better reconstruction, a set of linear transform measurements by using 2D DCT which are lowpass, acquired in zigzag order just like in JPEG can aid reconstruction significantly.

Yuan et al. [35] proposed that LL-DCT-ZZ measurements can be reconstructed back using Compressive Sensing reconstruction algorithms and showed that the scheme achieved better performance for SSIM in comparison to JPEG.

Zammit et al. [36] used block boundary variation for allocation of measurement rate. The rate allocation method is tested against both using deterministic DCT dictionaries and DAMP based Deep CS recovery. The method is simple and hardware friendly for implementation. How ever the method does not perform well especially at lower measurement rates.

Chen et al. [37] proposed a method of rate allocation based on distortion minimization. Sampling rate is allocated based on analytical function that minimizes the predicted distortion of the image block by using one of exponential/ logarithmic or polynomial model. The method introduces lot of complexity at decoder end. If the rate allocation happens on receiver, then a feedback loop of additional overhead is required for sensing the image. In recent past Adaptive rate allocation is used in conjunction with Deep compressive sensing and end to end parameters are learned, along with sampling matrices.

CASNET [9] proposes an adaptive rate allocation and solves the problem of different sampling matrices, by learning a huge unified sampling dictionary. Sampling matrix for any measurement rate is taken as a submatrix with first n*n

submatrix from top left corner. The huge sampling matrix is initialized by eigen values of training set and later learned during training phase. CASNET allocates saliency-based rate using a CNN network. Measurements are adjusted based on an algorithm that converges based on various saliency scores of the blocks. Though the network solves the problem of adaptive rate allocation, CASNET introduces complexity on encoder side of CS, which will be a challenge in sensor-based networks which generally would not have compute power. Sometimes the saliency-based rate allocation takes lot of iterations before converging. CASNET also has challenges with generalizability of Unified sampling matrix, as it is primarily based on eigen values of training data set and is tested against only natural images.

IV. PROPOSED ADAPTIVE RATE ALLOCATION ALGORITHM

Taking inspiration from LL-DCT-ZZ algorithm and using edge information at each block as a prior, the proposed algorithm allocates adoptive measurement rate per block. The proposed algorithm is first tested against 2D DCT dictionaries for effectiveness, as the recovery time is in milliseconds (real time). The aim is to have minimal complexity introduced at encoder side in adaptive rate allocation as well as the time taken to allocate measurement rate is minimal. Figure 2 shows the flow diagram of proposed algorithm, both at encoder as well as decoder side. Encoder splits the image into blocks and take measurements either using 2D DCT or learned measurement matrix. Measurement information is also passed along with rate information to decoder. Inverse CS is conducted per block based on rate allocation. Recovered image is formed by combining all the recovered blocks.

Image under consideration is divided into L blocks of B*B size as in below equation 5. Padding with 0 intensities on borders is used to make the image dividable into B*B blocks. W and H represents Width and Height of the image respectively.

$$L = \lceil W/B \rceil * \left\lceil {}^{H}/_{B} \right\rceil \tag{5}$$

A. EDGE BASED ADAPTIVE RATE ALLOCATION ALGORITHM

Given Image I_0, the edges are calculated with the images across the blocks by gaussian blur followed by canny edge detection as shown in Figure 1.

Rate allocation per block S_i is then calculated by the equation 6.

$$S_i = S_m + ae_i \tag{6}$$

where S_m is the minimum measurement rate for a block with 0 edges. e_i represents the edge pixel ratio with in the block. a represents the scaling factor. Calculation of each of these terms is elaborated in following equations.

S_m can be calculated from equation 7.

$$S_m = rS_0 \; where \; 0 < r < 1 \tag{7}$$

where S_0 is the overall measurement rate we want to achieve, r is a factor taken in between 0 and 1.

$$e_i = n_e/n_i \tag{8}$$

e_i represents the edge pixel ration with in the block, calculated by equation 8, i.e. total number of edge pixels n_e within the block by total number of pixels n_i in the block.

FIGURE 1. Edge detection across blocks using canny edge detection.

In Equation 6 a represents the scaling factor and is calculated as shown in equation 9.

$$a = L * (S_0 - S_m) / \sum e_i \tag{9}$$

L here represents the number of blocks in the image.

Rate allocation happens in 4 steps on encoder side with low complexity.

Step 1: Edge detection per block is done using Gaussian blur followed by canny edge detector. This ensures that the edges calculated are robust to noise.

Step 2: Minimum rate allocation for block S_m is selected.

Step 3: Block based adjustments based on edge information are calculated as per equation 6

Step 4: Remaining measurements S_a are readjusted to top edge information contained blocks as per equation 10 &11

$$S_a = S_0 - \sum S_i \tag{10}$$

$$A_d = \lceil S_a/m_1 \rceil \tag{11}$$

where A_d shows the measurement % to be adjusted, m_1 is the number of measurements that represent 1% for the given block size. For example, for a block size of 32*32, m_1 is around 10 measurements. The number A_d increases 1% measurements per block in the descending order of edge ratio. Meaning if A_d = n then n blocks with heist number of edge pixels in the descending order will get 1% increase in the measurement rate.

Initially r is taken as 0.5 and then different experiments are conducted by varying r value and effectiveness is measured. Measurement and recovery results of the rate allocation algorithm is presented in the next section

B. WEIGHTED EDGE BASED ADAPTIVE RATE ALLOCATION ALGORITHM

The algorithm proposed in previous section is improved by adding extra weight to edge pixels present in the border of the block.

Edge is an important characteristic in an image, which represents rapid changes in the intensity values. Allocating a greater number of measurements based on number of edge pixels present with in the block is effective, as the scheme allocates more measurements to block containing more edges. The presence of edge pixel in the border of a block has a special significance, as there is a high probability of the edge continuing into adjacent block. These pixels carry extra information beyond the block and often considering them equal to other edge pixel can cause undesired effects like blocking artifacts, after recovery.

In order to better address blocking artifacts due to block-based processing, the scheme allocates extra measurements based on number of border edge pixels present in the block according to equation 12

$$S_i = S_m + ae_i + n * \left({}^{e_b}/_{e_i}\right) \tag{12}$$

Here e_b represents edge pixels in border in i^{th} block and e_i is number of edge pixels in i^{th} block. 0<n<3, is a small multiplication factor to add additional weight.

For simplicity, we took n=1 and conducted the experiments.

Due to this special consideration for border edge pixels, sometimes, depending on the image as well as block size the measurement rate is greater than 100%. But taking 100% measurement rate does not make any sense in case of CS. So, the measurement rate is capped at 90% as a threshold in case of measurement rate going beyond 90%. Remaining adjustments shown in step 4 are calculated and adjusted as per equation 10 & 11.

Figure 10 shows the representation of block of image. Yellow areas represent edge pixels e_i, and areas in light brown represent edge pixels in border e_b.

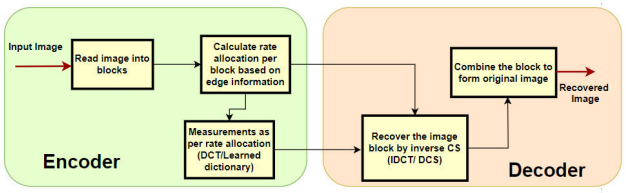

FIGURE 2. Flow diagram of adaptive block based compressive sensing based on edge information.

Algorithm1 and 2 below details out the proposed edge-based rate allocation algorithms

Algorithm 1 Edge Based Rate Allocation (EARA)

Input: Image I, block size B, compression factor S, Algorithms used for reconstruction = {IDCT2| CASNET}.

Output: Image I_o is sensed through EARA algorithm and reconstructed using the reconstruction algorithms

1 Divide the image I into L Block of size B* B each $L = \lceil W/B \rceil * \lceil H/B \rceil$
2 Blur the image block using Gaussian Blur
3 Detect the edges using Canny edge detector
4 Calculate minimum allocation rate S_m by setting rate factor r
5 For each block b in blocks:
6 Calculate edge pixels ratio $e_i = n_e/n_i$
7 $\sum e+ = e_i$
8 Calculate the edge factor $a = L * (S_0 - S_m)/\sum e_i$
9 Measurement per block $S_i = S_m + ae_i$
10 Complete the remaining adjustments
11 Collect S_i measurements per block
12 Transmit measurements & number of measurements per block to decoder
13 Reconstruct I_o at the output per reconstruction algorithm

Algorithm 2 Weighted Edge Based Rate Allocation (WEARA)

Input: Image I, block size B, compression factor S, Algorithms used for reconstruction = {IDCT2| CASNET}.

Output: Image I_o is sensed through WEARA algorithm and reconstructed using the reconstruction algorithms

1 Divide the image I into L Block of size B*B each $L = \lceil W/B \rceil * \lceil H/B \rceil$
2 Blur the image block using Gaussian Blur
3 Detect the edges using Canny edge detector
4 Calculate minimum allocation rate S_m by setting rate factor r
5 For each block b in blocks:
6 Calculate edge pixels ratio $e_i = n_e/n_i$
7 Calculate edge pixels at block boundaries
8 $\sum e+ = e_i$
9 Calculate the edge factor $a = L * (S_0 - S_m)/\sum e_i$
10 Measurements $S_i = S_m + ae_i + n * (e_b/e_i)$
11 Adjust measurements with max cap of 90%
12 Collect S_i measurements per block
13 Transmit measurements to decoder
14 Reconstruct I_o at the output per reconstruction algorithm

V. SENSING AND RECOVERY AND RESULTS ANALYSIS

A. RECOVERY USING DCT / IDCT DICTIONARIES

The proposed algorithms are first tested using 2D-DCT dictionaries and IDCT is applied at the decoder end for recovering the original image. For instance, Monarch image as shown in figure 1, when conducted experiments with 32*32 block size, to achieve 10% measurement rate, a block with highest edge pixel ratio got 18% measurement rate while the block with no edge pixel got 5% measurement rate since r is taken as 0.5 in the first iteration.

Once the measurement rate is allocated per block, DCT is applied on each block of the image. First n coefficients as per

FIGURE 3. Parrots, camara man, peppers, boats, barbara, monarch, house and forman images (256 X 256) used for testing.

TABLE 1. Avg PSNR/SSIM for different IDCT based methods.

Measurement rate	10%		20%		30%		40%	
Methodology	PSNR (dB)	SSIM	PSNR (dB)	SSIM	PSNR (dB)	SSIM	PSNR (dB)	SSIM
AL-DCT-DD [36]	27.67	0.8131	30.78	0.8865	33.19	0.9223	35.22	0.9446
AL-DCT-BBV [36]	27.28	0.7982	30.64	0.8823	33.34	0.9226	35.57	0.9459
L-DCT-ZZ [35]	26.92	0.803	29.67	0.8795	31.82	0.9182	33.71	0.9429
EARA (ours)	28.43	0.8451	31.37	**0.9296**	34.59	**0.9249**	37.59	**0.9618**
WEARA (ours)	**28.47**	**0.8457**	**31.47**	0.9295	**34.74**	0.9422	**38.6**	0.9612

the measurement rate allocated are captured in zig zag order as shown in figure 4. Set 11 Dataset is used for evaluation. Set11 consists of 11 gray scale images of size 256* 256. 8 images of size 256 * 256 each from data set 'set11' are used for evaluations. The images used are shown in figure 3. Each image is tested for different measurement rates from 0.04, 0.1,0.2, 0.3, 0.4, 0.5.

The effect of rate factor r is shown in figure 5 for different measurement rates. Set of 8 images in Figure 3 are taken, WEARA based rate allocation is performed for 32*32 blocks with multiplication factor n is taken as 2. DCT/ IDCT is used for sensing and reconstruction. Average PSNR values of recovered images. At lower measurement rates, small rate factor (r=0.3) has more performance by small margin, as the measurement rate increases, small rate factor is not effective. Effectiveness of rate factor increases till r=0.5 and has counter impact once r > 0.5 onwards. Taking these factors into consideration, r is fixed at 0.5.

The comparison of Average PNSR using proposed methods with AL-DCT-BBV method [36] and EFM-Exponential method [37]. Clearly proposed methods outperform the PSNR values by a large margin. Effectiveness of weighted edge-based rate allocation (WEARA) is a small margin in lower measurement rates, but shows clear margin in higher measurement rates. Time taken for recovery at any measurement rate in this setting is in range of 50-65 milli seconds, making it real time reconstruction.

Table 1 shows the comparison of Average PSNR and SSIM obtained by similar DCT/IDCT based recovery methods with the proposed Edge pixel-based methods. Clearly proposed algorithms have better PSNR and SSIM values for wide range of CS ratios. Comparing between the two proposed methods as shown in Figure 6, PSNR of WEARA is better than EARA algorithm. SSIM values are very close and at higher CS ratios

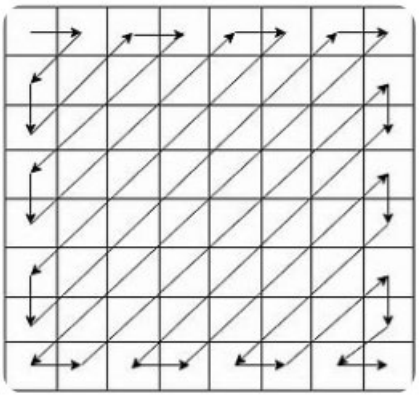

FIGURE 4. Zigzag order of reading DCT coefficients.

better SSIM is observed in EARA based algorithm without using weights.

Figure 13 shows the comparison of Parrot recovered image at different rates of measurement using WEARA algorithm using DCT. Subjective quality of recovered image can be compared by understanding texture features around the eye of the parrot.

B. RECOVERY USING CASNET

In the recent past, many State-of-the-Art algorithms are proposed in CS recovery based on Deep learning based compressed sensing. In this section we test the proposed algorithms in conjunction with the work done by Chen et al. *[9]*, the deep neural network they proposed is called CASNet. CASNET has majorly 3 sub networks. Sampling Subnet (SS), Initialization subnet (IS) and Deep Recovery subnet (RS). Sampling subnet has a neural network which creates the

TABLE 2. Average PSNR/SSIM for Set 11 by various Deep compressed sensing methods.

CS method	4%	10%	25%	30%	40%	50%
COAST [28]	–/–	0.03/0.8946	–/–	36.35/0.9618	–/–	40.32/0.9804
BCSNET [8]	24.90/0.7531	29.42/0.8673	34.20/0.9408	35.63/0.9495	36.68/0.9667	39.58/0.9734
CSNet+ [19]	24.83/0.7480	28.34/0.8580	33.34/0.9387	34.27/0.9492	36.44/0.9690	38.47/0.9796
ISTA-Net+ [23]	21.32/0.6037	26.64/0.8087	32.59/0.9254	33.68/0.9352	35.97/0.9544	38.11/0.9707
SCSNet [38]	24.29/0.7589	28.52/0.8616	33.43/0.9373	34.64/0.9511	36.92/0.9666	39.01/0.9769
AMP-Net [24]	25.14/0.7701	29.42/0.8782	34.60/0.9469	35.91/0.9576	38.25/0.9714	40.26/0.9786
OPINE-Net+ [21]	25.69/0.7920	29.81/0.8904	34.86/0.9509	35.79/0.9541	37.96/0.9633	40.19/0.9800
CASNet [9]	26.41/0.8153	30.36/0.9014	35.67/0.9591	36.92/0.9662	39.04/0.9760	40.93/0.9826
WEARA+ CASNet (ours)	27.58/0.8249	31.39/0.9087	36.71/0.9559	38.19/0.9644	40.63/0.9766	41.11/0.9764

saliency map for the image block and allocates measurement rate for it. To get to the overall desired measurement rate it uses Block Ratio Aggregation strategy (BRA). We replace the Sampling subnet with the proposed algorithm for measurement rate allocation. For recovery remaining 2 subnets are used as is.

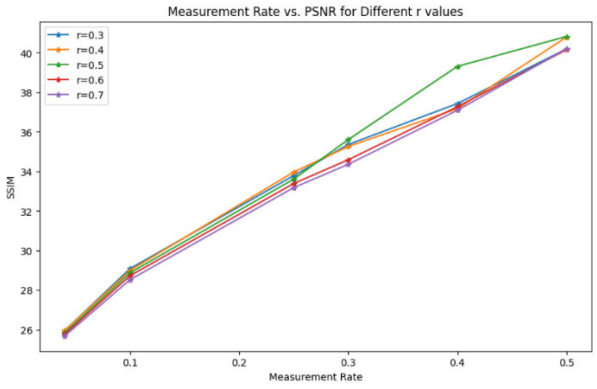

FIGURE 5. Effect of r value on different measurement rates.

The experiment is done to check the adaptability of the proposed algorithm with any effective custom recovery technique.

Unlike many other Deep compressed sensing techniques, in which models are trained separately for different measurement rates, CASNET uses a Unified learnable Generating matrix A, from which first q rows are used as sampling matrix based on sampling rate q. A is initialized by using Singular vale Decomposition of training set and later learned as part of training process.

At the recovery end, initial estimate of the recovered signal is done by using the equation below

$$\hat{x}_i^{(0)} = A_{qi}^T y_i \tag{13}$$

Recovery is iteratively done by using proximal gradient descent implemented through CNN, by solving equations 14 & 15

$$z^{(k)} = \widehat{\boldsymbol{x}}^{(k-1)} - \rho\phi^T\left(\phi\widehat{\boldsymbol{x}}^{(k-1)} - y\right) \tag{14}$$

$$\hat{x}^{(k)} = \underset{x}{argmin}\frac{1}{2}\left\|\left(x - z^{(k)}\right)\right\|_2^2 + \lambda R(x) \tag{15}$$

where k represents the iteration index of PGD and ρ denotes the step size. Equation 14 is general step in gradient descent, and equation 15 shows the proximal mapping step. λR represents regularization term.

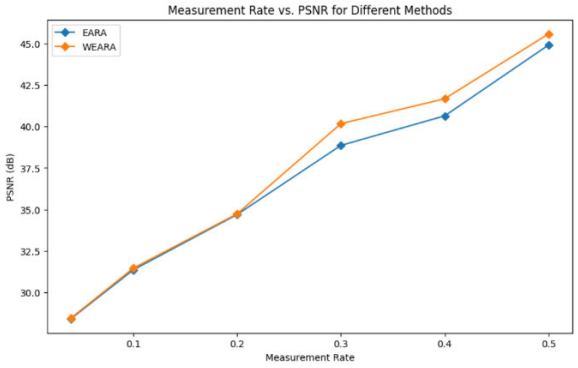

FIGURE 6. Avg PSNR of different methods, $r = 0.5$ for proposed methods.

We used the Weighted edge-based rate allocation algorithms for measurement rate allocation with r=0.5 and n=1 and then used the rest of the implementation of CASNet as is. Experiments are conducted with set 11 dataset with different measurement rates. The comparison of Weighted edge-based Rate allocation method using CASNet against other 8 state of the art methods are shown in Table 2. Proposed method in conjunction with CASNet outperform CASNET and other methods, with consistent higher PSNR across all measurement rates. SSIM values are generally better, except for 25% and 30% measurement rates, where SSIM of CASNet is better by a very small margin. Figure 7 shows and compares the

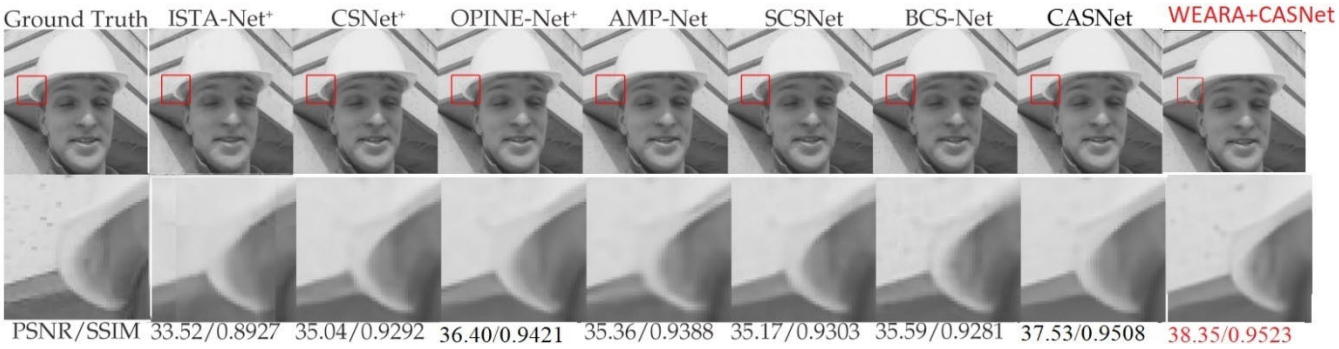

FIGURE 7. Forman visual comparison after recovery by various methods.

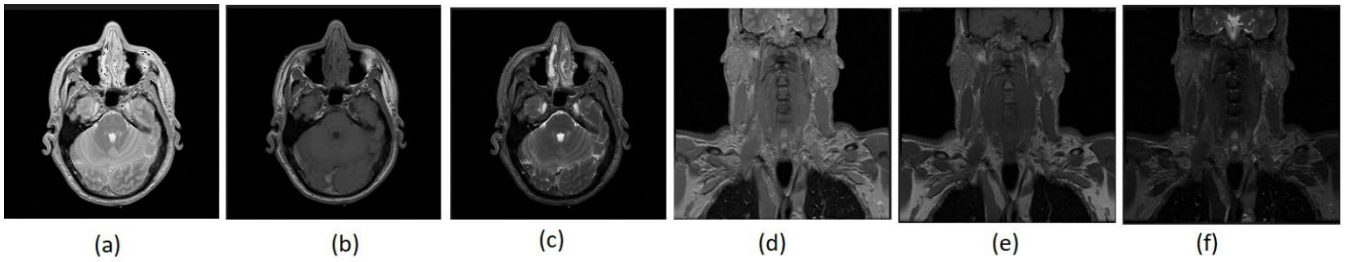

FIGURE 8. Medical images used for evaluation (a) Human head subset - proton density (b) T1 Human head subset (c) T2 human head subset (d) Thorax subset -Proton density (e)T1- Thorax subset (f) T2- Thorax subset.

visual results of recovered image of foreman image using different state of the art recovery techniques.

C. RESULTS FOR MEDICAL IMAGES

Proposed rate allocation methods are tested against 6 medical images taken from Visible human project initiated by the National Library of Medicine (NLM). Images in Visible Human Project are openly accessible for research purposes. The Dataset consists of CT,MRI and Cryosection of human subjects [39]. T1, T2 and Protein density images of Head Subset and Thorax Subset respectively are taken into consideration. Each image is of size 256*256. The images are shown in Figure 8.

Medical images are sensed and reconstructed using proposed algorithms, both with deterministic as well as CASNet implementations.

Unlike the natural images, medical images have different patterns exhibited. In general, MRI based scans are sparser and more compressible when Fourier dictionaries are used. But to check the generality of the proposed algorithm and easier comparison, we used DCT based deterministic dictionaries for these medical images.

The medical images are sampled by using 32 * 32 blocks with WEARA as well as EARA algorithms as part of our experiments. Table 3 shows the results of PSNR/SSIM of 6 medical images using WEARA algorithm using DCT/IDCT recovery.

Figure 9 shows the visual comparison of recovered image which is sampled using WEARA using IDCT at 30% sampling rate. Figure 11 shows the detailed view of highlighted areas in figure 9.

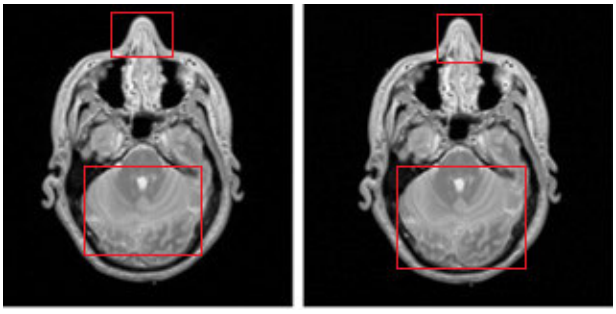

FIGURE 9. Comparison of recovered image (left) and original image for 30% sampling of proton head sub image (PSNR/SSIM: 31.64/0.9642).

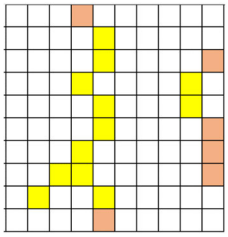

FIGURE 10. Representation of edge pixels and border edge pixel in the block.

At 40% or 50% measurement rates the distortions in the detail are small compared to 30% or lower. Table 4 shows

TABLE 3. Average PSNR/SSIM with WEARA for 6 medical images using DCT/IDCT dictionaries.

Image	4%	10%	20%	30%	40%	50%
Head sub image - PD	23.46/ 0.7921	26.30/ 0.8875	29.03/ 0.9404	31.64/ 0.9642	34.10/ 0.9765	40.40/ 0.9878
Head sub image - T1	28.83/ 0.8641	32.56/ 0.9355	37.50/ 0.9721	41.91/ 0.9858	45.68/ 0.9918	50.16/ 0.9980
Head sub image - T2	28.58/ 0.8456	31.69/ 0.9226	35.12/ 0.9597	38.28/ 0.9756	41.23/ 0.9850	48.40/ 0.9941
Thorax sub image - PD	27.70/ 0.7205	30.54/ 0.8406	33.56/ 0.9123	36.02/ 0.9453	38.38/ 0.9639	42.55/ 0.9815
Thorax sub image - T1	30.35/ 0.7836	33.52/ 0.8814	36.59/ 0.9328	38.95/ 0.9572	41.35/ 0.9725	44.07/ 0.9834
Thorax sub image T2	31.91/ 0.7737	34.19/ 0.8527	36.61/ 0.9106	40.22/ 0.9975	43.28/ 0.9801	42.06/ 0.9717

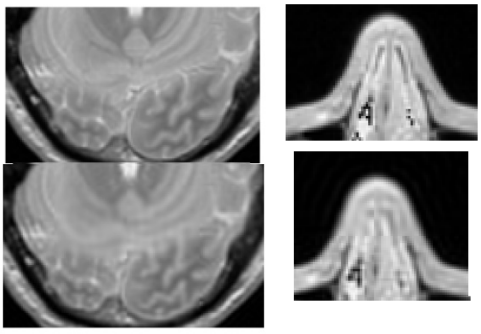

FIGURE 11. Comparison of differences in highlighted spots. Ground reality(upper) recovered (lower).

the comparison of computational complexity using DCT dictionaries. Clearly other state of art methods has Millions of parameters to be trained with high compute machines like GPUs.

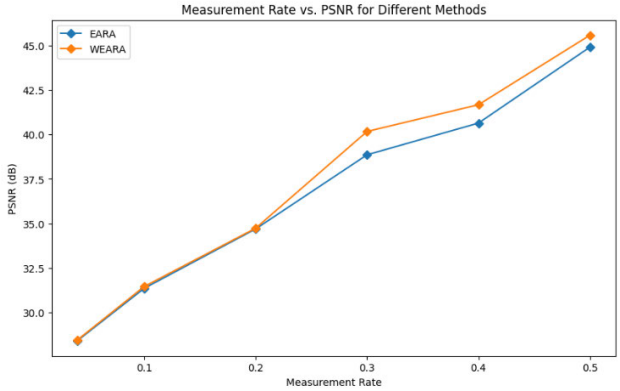

FIGURE 12. Average PSNR for r =0.5 for EARA and WEARA rate allocation on 6 medical images using DCT.

FIGURE 13. Parrot recovered using IDCT with WEARA for 10, 25, 30 and 40% measurement rate- PSNR(DB)/SSIM values shown at bottom.

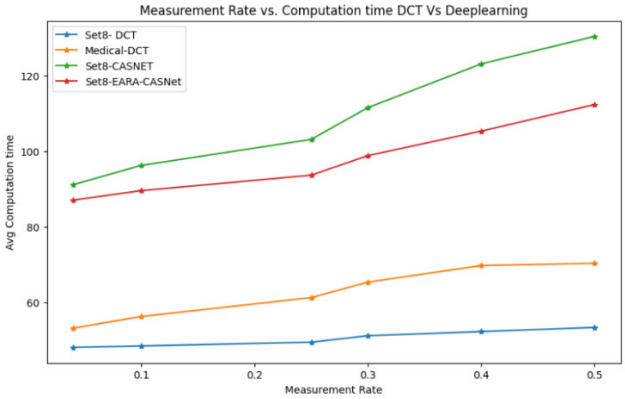

FIGURE 14. Comparison of computation time using DCT vs Deep learning-based recovery.

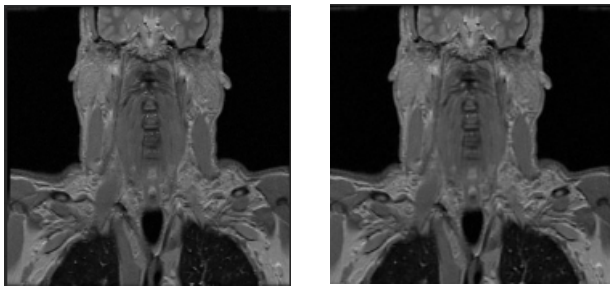

FIGURE 15. Thorax Proton density image original (left), recovered from 30% measurement using CASNET PSNR(DB)/SSIM: 36.05/0.9470.

Figure 12 shows the comparison average PSNR of EARA and WEARA algorithms for recovery of 6 medical images for different measurement rates. At lower measurement rates the advantage of weighted rate allocation is very small, however from measurement rates $>$ 20% the advantage in PSNR is clearly visible using WEARA algorithm.

Figure 14 shows the image recovered using CASNET with WEARA algorithm at 30% measurement rate. At measurement rates lesser then 10% (1%, 4%) blocking artifacts are clearly observed in medical images using both CASNET as well as 2D DCT dictionaries. From 10% onwards the

TABLE 4. Comparison of computational complexity.

Method	Type of CS recovery	Uses Deep learning	GPU required	No of params to be trained (M)
EARA/WEAR A with DCT based CS	2D DCT/IDCT	X	X	NA
CASNET [9]	Learned dictionary/ Proximal Gradient decent	√	√	16.9
AMP-Net [24]	Learned dictionary/ AMP based recovery	√	√	6.8

recovered signal has understandable details when compared visually. Comparison of recovery time using simple DCT based dictionaries vs Model based deep learning is conducted. Time measured for CASNET based deep learning model is obtained by using L4 GPU machine. Whereas the time obtained using DCT dictionaries is by using 8 core, 1TB CPU machine without using expensive GPUs.

The results are represented in Figure 15. Clearly DCT based sensing and recovery took much less time for both medical and natural images when compared to Deep learning recovery. In case of CASNET or EARA based (for measurement allocation) CASNET for reconstruction computational time is higher compared to DCT dictionaries. Hence DCT dictionaries can ensure real time reconstruction at all measurement rates.

VI. CONCLUSION AND FUTURE WORK

Two adoptive rate allocation ABCS algorithms are proposed based on edge information in each block of the image. In both of the algorithms simple edge detection techniques and linear equations to calculate the rate allocation per block are used. Since rate allocation is linear and simple, it is much suitable for sensors which generally has less compute power.

The proposed algorithms are tested against set of 8 natural images using deterministic DCT dictionaries to understand the effectiveness. Time taken to recover original image is in the range of 50 to 65 milliseconds, making it real time reconstruction.

The proposed algorithm is also tested using CASNET where measurement matrix is taken as a submatrix from a unified learned measurement matrix. Recovery of image using CASNET using the proposed rate allocation techniques have outperformed other state of the art techniques.

To understand the generalizability of the algorithm, it is tested against a set of 6 medical images with different measurement rates with DCT/ IDCT as well as CASNET recovery. In both cases the recovered images exhibited high PSNR and SSIM values, showing the adoptability of the proposed algorithms.

Comparison of recovery time and computational complexity using DCT vs trained dictionaries of various methods is also presented.

In future, the proposed algorithms can also be compared for video encoding applications. Apart of edge only information, consideration of texture information in combination to edge information might further enhance the performance across wide range of images. This can be improved as part of future work. Comparison of proposed method against different deterministic measurement matrices like Bernoulli/ Fourier can also give valuable insights and might help adopting the right measurement matrix for real-time high-quality recovery.

REFERENCES

[1] E. J. Candes, J. Romberg, and T. Tao, "Robust uncertainty principles: Exact signal reconstruction from highly incomplete frequency information," *IEEE Trans. Inf. Theory*, vol. 52, no. 2, pp. 489–509, Feb. 2006.
[2] Y. Tsaig and D. L. Donoho, "Extensions of compressed sensing," *Signal Process.*, vol. 86, no. 3, pp. 549–571, Mar. 2006.
[3] S. Zhou, Y. He, Y. Liu, C. Li, and J. Zhang, "Multi-channel deep networks for block-based image compressive sensing," *IEEE Trans. Multimedia*, vol. 23, pp. 2627–2640, 2021.
[4] P. Sermwuthisarn, S. Auethavekiat, and V. Patanavijit, "A fast image recovery using compressive sensing technique with block based orthogonal matching pursuit," in *Proc. Int. Symp. Intell. Signal Process. Commun. Syst. (ISPACS)*, Jan. 2009, pp. 212–215.
[5] S. K. Sahoo and A. Makur, "Signal recovery from random measurements via extended orthogonal matching pursuit," *IEEE Trans. Signal Process.*, vol. 63, no. 10, pp. 2572–2581, May 2015.
[6] D. L. Donoho, "Compressed sensing," *IEEE Trans. Inf. Theory*, vol. 52, no. 4, pp. 1289–1306, Apr. 2006.
[7] R. Monika, D. Samiappan, and R. Kumar, "Adaptive block compressed sensing—A technological analysis and survey on challenges, innovation directions and applications," *Multimedia Tools Appl.*, vol. 80, no. 3, pp. 4751–4768, Jan. 2021.
[8] S. Zhou, Y. He, Y. Liu, C. Li, and J. Zhang, "Multi-channel deep networks for block-based image compressive sensing," *IEEE Trans. Multimedia*, vol. 23, pp. 2627–2640, 2021.
[9] B. Chen and J. Zhang, "Content-aware scalable deep compressed sensing," *IEEE Trans. Image Process.*, vol. 31, pp. 5412–5426, 2022.
[10] J. Romberg, "Imaging via compressive sampling," *IEEE Signal Process. Mag.*, vol. 25, no. 2, pp. 14–20, Mar. 2008.
[11] A. Beck and M. Teboulle, "A fast iterative shrinkage-thresholding algorithm for linear inverse problems," *SIAM J. Imag. Sci.*, vol. 2, no. 1, pp. 183–202, Jan. 2009.
[12] D. L. Donoho, A. Maleki, and A. Montanari, "Message passing algorithms for compressed sensing: I. Motivation and construction," in *Proc. IEEE Inf. Theory Workshop Inf. Theory (ITW)*, Cairo, Egypt, Jan. 2010, pp. 1–5.
[13] S. Boyd, "Distributed optimization and statistical learning via the alternating direction method of multipliers," *Found. Trends Mach. Learn.*, vol. 3, no. 1, pp. 1–122, 2010.
[14] S. Ji and L. Carin, "Bayesian compressive sensing and projection optimization," in *Proc. 24th Int. Conf. Mach. Learn.*, Jun. 2007, pp. 377–384.
[15] D. Baron, S. Sarvotham, and R. G. Baraniuk, "Bayesian compressive sensing via belief propagation," *IEEE Trans. Signal Process.*, vol. 58, no. 1, pp. 269–280, Jan. 2010.
[16] S. Ji, Y. Xue, and L. Carin, "Bayesian compressive sensing," *IEEE Trans. Signal Process.*, vol. 56, no. 6, pp. 2346–2356, Jun. 2008.
[17] W. Guo and W. Yin, "EdgeCS: Edge guided compressive sensing reconstruction," in *Visual Communications and Image Processing*, vol. 7744. Bellingham, WA, USA: SPIE, 2011, pp. 192–201.
[18] M. Ran, W. Xia, Y. Huang, Z. Lu, P. Bao, Y. Liu, H. Sun, J. Zhou, and Y. Zhang, "MD-Recon-Net: A parallel dual-domain convolutional neural network for compressed sensing MRI," *IEEE Trans. Radiat. Plasma Med. Sci.*, vol. 5, no. 1, pp. 120–135, Jan. 2021.
[19] W. Shi, F. Jiang, S. Liu, and D. Zhao, "Image compressed sensing using convolutional neural network," *IEEE Trans. Image Process.*, vol. 29, pp. 88–375, 2019.

[20] M. B. Hossain, K.-C. Kwon, S. M. Imtiaz, O.-S. Nam, S.-H. Jeon, and N. Kim, "De-aliasing and accelerated sparse magnetic resonance image reconstruction using fully dense CNN with attention gates," *Bioengineering*, vol. 10, no. 1, p. 22, Dec. 2022.
[21] J. Zhang, C. Zhao, and W. Gao, "Optimization-inspired compact deep compressive sensing," *IEEE J. Sel. Topics Signal Process.*, vol. 14, no. 4, pp. 765–774, May 2020.
[22] Y. Yang, J. Sun, H. Li, and Z. Xu, "ADMM-CSNet: A deep learning approach for image compressive sensing," *IEEE Trans. Pattern Anal. Mach. Intell.*, vol. 42, no. 3, pp. 521–538, Mar. 2020.
[23] J. Zhang and B. Ghanem, "ISTA-Net: Interpretable optimization-inspired deep network for image compressive sensing," in *Proc. IEEE/CVF Conf. Comput. Vis. Pattern Recognit.*, Salt Lake City, UT, USA, Jun. 2018, pp. 1828–1837.
[24] Z. Zhang, Y. Liu, J. Liu, F. Wen, and C. Zhu, "AMP-Net: Denoising-based deep unfolding for compressive image sensing," *IEEE Trans. Image Process.*, vol. 30, pp. 1487–1500, 2021.
[25] V. Pavitra, V. B. S. S. I. Dutt, and G. V. S. R. Kumar, "Deep learning based compressive sensing for image reconstruction and inference," in *Proc. IEEE 7th Int. Conf. for Converg. Technol. (I CT)*, Mumbai, India, Apr. 2022, pp. 1–7.
[26] H. Yao, F. Dai, S. Zhang, Y. Zhang, Q. Tian, and C. Xu, "DR^{2}Net: Deep residual reconstruction network for image compressive sensing," *Neurocomputing*, vol. 359, pp. 483–493, Sep. 2019.
[27] W. Cui, S. Liu, F. Jiang, and D. Zhao, "Image compressed sensing using non-local neural network," *IEEE Trans. Multimedia*, vol. 25, pp. 816–830, 2023.
[28] D. You, J. Zhang, J. Xie, B. Chen, and S. Ma, "COAST: COntrollable arbitrary-sampling NeTwork for compressive sensing," *IEEE Trans. Image Process.*, vol. 30, pp. 6066–6080, 2021.
[29] Z. Gao, C. Xiong, L. Ding, and C. Zhou, "Image representation using block compressive sensing for compression applications," *J. Vis. Commun. Image Represent.*, vol. 24, no. 7, pp. 885–894, Oct. 2013.
[30] S. Zhu, B. Zeng, and M. Gabbouj, "Adaptive reweighted compressed sensing for image compression," in *Proc. IEEE Int. Symp. Circuits Syst. (ISCAS)*, Jun. 2014, pp. 1–4.
[31] J. Zhang, Q. Xiang, Y. Yin, C. Chen, and X. Luo, "Adaptive compressed sensing for wireless image sensor networks," *Multimedia Tools Appl.*, vol. 76, no. 3, pp. 4227–4242, Feb. 2017.
[32] R. Li, X. Duan, and Y. Lv, "Adaptive compressive sensing of images using error between blocks," *Int. J. Distrib. Sensor Netw.*, vol. 14, no. 6, Jun. 2018, Art. no. 155014771878175.
[33] F. Sun, D. Xiao, W. He, and R. Li, "Adaptive image compressive sensing using texture contrast," *Int. J. Digit. Multimedia Broadcast.*, vol. 2017, no. 1, pp. 1–10, 2017.
[34] S. Zhou, Z. Chen, Q. Zhong, and H. Li, "Block compressed sampling of image signals by saliency based adaptive partitioning," *Multimedia Tools Appl.*, vol. 78, no. 1, pp. 537–553, Jan. 2019.
[35] X. Yuan and R. Haimi-Cohen, "Image compression based on compressive sensing: End-to-end comparison with JPEG," 2017, *arXiv:1706.01000*.
[36] J. Zammit and I. J. Wassell, "Adaptive block compressive sensing: Toward a real-time and low-complexity implementation," *IEEE Access*, vol. 8, pp. 120999–121013, 2020.
[37] Q. Chen, D. Chen, and J. Gong, "Low-complexity adaptive sampling of block compressed sensing based on distortion minimization," *Sensors*, vol. 22, no. 13, p. 4806, Jun. 2022.
[38] W. Shi, F. Jiang, S. Liu, and D. Zhao, "Scalable convolutional neural network for image compressed sensing," in *Proc. IEEE/CVF Conf. Comput. Vis. Pattern Recognit.*, 2019.
[39] Internet. (2024). *National Library of Madicine*. National Center for Biotechnology Information. [Online]. Available: https://www.nlm.nih.gov/research/visible/animations.html

V. PAVITRA (Member, IEEE) received the B.Tech. degree in electronics and communications from the Bapatla Engineering College, Acharya Nagarjuna University, Andhra Pradesh, India, in 2006, and the M.Tech. degree in digital electronics and communication systems from GNITS, Jawaharlal Technological University, Telangana, India. She is currently pursuing the Ph.D. degree with GITAM University, Vishakhapatnam, Andhra Pradesh, India. Her research interests include compressive sensing, wireless networks, deep learning, and generative AI.

V. B. S. SRILATHA INDIRA DUTT received the B.Tech. degree from the Velagapudi Ramakrishna Siddartha Engineering College, Andhra Pradesh, India, and the M.Tech. and Ph.D. degrees from Andhra University College of Engineering (AUCE), Andhra University, India. She is currently a Professor with the Department of Electrical, Electronics and Communication Engineering, GITAM Deemed to be University, Visakhapatnam, Andhra Pradesh. She has published more than 100 research articles in reputed journals and conferences. Her research interests include global navigation satellite systems, wireless communications, and deep learning.